Economic Geology
Vol. 88, 1993, pp. 1977–1988

A Capless 350°C Flow Zone Model to Explain Megaplumes, Salinity Variations, and High-Temperature Veins in Ridge Axis Hydrothermal Systems

L. M. CATHLES

Department of Geological Sciences, Cornell University, Ithaca, New York 14853

Abstract

The physical characteristics of the deeper (>~1.5 km), higher temperature (≥~350°C) parts of typical ridge axis hydrothermal systems are determined by combining selected observations with equations expressing the conservation of mass, energy, and momentum. The observations are: the ~350°C temperature of venting solutions, the variation of vent salinities from half to twice that of seawater, the <10-yr residence time of seawater from the time it is heated to temperatures >150°C to discharge, the variation in black smoker venting rates from normal to megaplume, and an intrusion geometry consistent with seismic and other data. With these observations the conservation equations predict: a ~3.4-m-wide, 330-mD, 350°C flow zone is separated by ~180 m from the hot (1,200°C) parts of the axial intrusion. High fluid velocities in the thin 350°C flow zone make it the most resistive element in the convection circuit. Tectonic and magmatic disturbances can increase the permeability of the thin flow zone by two to three orders of magnitude. When this occurs discharge of 350°C waters increases to megaplume rates for the several days that is required for the width of the flow zone to contract and the heat stored in the formerly wider flow zone to be discharged into the megaplume. The rate of discharge then returns to premegaplume levels. Cracking allows seawater to invade hot areas of the thermal boundary layer and undergo phase separation. Cracking 70 percent of the thermal boundary layer produces sufficient volumes of brine, and returns and recondenses sufficient low-salinity vapor in the thin 350°C flow zone, to reduce the salinity of the flow zone waters to half seawater levels. Flushing of the thermal boundary layer brines by the later migration of the flow zone into the thermal boundary layer results in a complimentary increase in flow zone (and discharge) salinity to twice seawater levels. Cl-rich veins observed in the Bushveld have lengths, widths, and spacings similar to those required to produce these salinity variations. The model suggests new ways to combine field observations for massive sulfide exploration. Definitive tests of the model could be provided by drilling the near-ridge environment to depths of ~2 km.

Introduction

OVER the last decade and a half a number of generalizations have emerged from studies of ridge axis hydrothermal systems: the temperatures of black smoker venting are stable and almost always about 350°C (e.g., Campbell et al., 1988a, b). Higher temperature discharges have been found, but they are rare (e.g., Tivey et al., 1990). Black smokers occur along up to ~12-km-long eruptive fissures at the ridge axis, in the center of the inner rift. Commonly, three to four black smoker clusters and a number of white smokers are almost perfectly aligned along the linear fracture (e.g., Francheteau and Ballard, 1983). Where midocean ridges have been surveyed seismically, the hot intrusions appear to be ~4-km-wide, ridge-parallel stocks with tops at a few kilometers' depth and bases at the Moho (McClain et al., 1985; Dietrick, 1987). Magma is concentrated in a small chamber at the top of the intrusion which has at most a few percent partial melt (Macdonald, 1989).

Typical discharge rates of 350°C fluid from a single black smoker site are 75 to 150 kg/s. Even at these normal rates the thermal discharge is greater than can be sustained by steady sea-floor spreading (Macdonald et al., 1980; Converse, 1984; Baker et al., 1989). Inactive axial vents have been found. For both reasons hydrothermal venting must be time variable. That there can be spectacular variations in discharge rate is indicated by the discovery of a huge thermal cloud with heavy entrained particulate matter on the Juan de Fuca Ridge in August 1986. The 1,000-m height of the plume above the sea floor, its volume, and the size and density of its entrained particulates indicate that 0.03 to 0.08 km^3 of 350°C water (up to 1.3×10^{17} joules or 2.88×10^{16} cal) must have vented from a 200- to 2,000-m-long fissure in 2 to 20 days (Baker et al., 1989) at ~250 times the normal rate of discharge (Cann and Strens, 1989). High-temperature discharge was occurring along this Cleft segment of the Juan de Fuca Ridge before and after the megaplume event (Baker, 1990; Baker and Lupton, 1990).

Radiogenic isotopes indicate that the residence time of seawater in midocean ridge hydrothermal systems venting at normal rates is less than 10 yr from

0361-0128/93/1518/1977-12$4.00

the point where temperatures of ~150°C are encountered to the surface (Kadko and Moore, 1988). The salinity of venting solutions is on average that of seawater but varies from 40 to 130 percent seawater salinity in specific vents (see excellent review in Bischoff, 1989; Von Damm, 1990). Fluid inclusions and isotopic differences between mineral phases indicate that massive sulfide deposits also formed at ~350°C temperatures and experienced variations in salinity from half to twice that of seawater (e.g., Pisutha-Arnond and Ohmoto, 1983). The trace element chemistry of vent waters is complex and reflects phase separation, the later mixing of the vapor and brine components, chemical reequilibration of components with rock, and a small contribution from the precipitation of Cl minerals (e.g., Berndt and Seyfried, 1990). High-temperature (>600°C) veins containing Cl-rich amphiboles that have no alteration halos, and somewhat lower temperature veins containing hydrothermal plagioclase and fluid inclusions with homogenization temperatures between 300° and 600°C that have only narrow alteration halos have been observed in gabbro complexes such as the Bushveld (Schiffries and Skinner, 1987). Similar veins and Cl-rich amphiboles have been observed in gabbros recovered from the ocean floor (Vanko, 1986; Kelly and Delaney, 1987).

A number of explanations for these observations have been offered. The stocklike intrusion geometry requires convective pore water circulation to Moho depths (Fehn et al., 1983; Morton and Sleep, 1985). The pattern of surface heat flow (Fehn et al., 1983) and the profile of oxygen and strontium isotope alteration in ophiolites (Gregory and Taylor, 1981; Cathles, 1983) confirm flow to Moho depth. The ubiquitous and stable 350°C venting has been recognized as a feature that must be explained by any model. Cathles (1983) suggested that 350°C venting required interaction of the hydrothermal system with magma and a ~350°C cutoff in permeability caused by the rapid dissolution of fracture contact points and fracture closure at higher temperatures. Bischoff and Rosenbauer (1989) have suggested that ~360°C is the temperature at which seawater circulation downward toward a convecting brine layer or hot rock expands and turns around to return to the surface. However, calculations suggest that such changes in the properties of water cannot regulate the temperature if the near-vertical sides of narrow magma chambers are exposed to hydrothermal circulation (Cathles, 1983).

Salinity increases cannot be related to simple boiling because vent solutions show little evidence of gas segregation into a vapor phase (Von Damm and Bischoff, 1987). Cl-rich minerals whose precipitation and dissolution might control salinity variations have been investigated, but vent salinities different from seawater are the norm rather than the exception, and experiments indicate Cl-rich minerals can be formed only with difficulty (Bischoff and Rosenbauer, 1989). Bischoff and Rosenbauer (1989) have suggested that the variations in salinity are due to double diffusive convection. In their view, seawater convection occurs over a deeper brine convection cell. Mixing of seawater with the gas-depleted brine explains the high-salinity discharges; boiling of the brine and recondensation of the vapor in the overlying seawater system explains the low-salinity discharges. Such a layered convection could produce the ophiolite oxygen isotope profile.

Baker et al. (1989) proposed that the most likely explanation for megaplume discharges was the cataclysmic emptying of a reservoir of hot fluid stored in the axial crust. They noted that high-temperature reaction zones observed in the Troodos Massif could supply sufficient volumes of pore water to explain the Juan de Fuca megaplume if the porosities were ~10 percent. A ridge axis that is undergoing extension at centimeters per year seems a poor place to develop a seal, however, and if capped reservoirs did develop at ocean ridges, the venting should frequently be off axis. Cann and Strens (1989) noted the absence of evidence for an appropriate cap at midocean ridges or in the Troodos Massif. They proposed instead that a resistive cap and cylindrical shell grows in and around the discharge zone until near-surface inflow and mixing of discharging hydrothermal fluids and seawater is eliminated. Temperature and buoyancy forces then build toward lithospheric levels within the cylinder until rupturing and megaplume discharge occurs. The system then reclogs by seawater mixing, reheats, and ruptures again. Cann and Strens' model of megaplume discharge at Juan de Fuca rates requires recharge permeabilities of ~10 D and a 200-m^2 breccia zone (50% porosity and 5-cm-diam particle size) in the discharge areas. The Cann and Strens' discharge cylinder sits on the flat top of the axial intrusion heat source in the upper 1.5 km of the oceanic crust. Heat is scavenged from the top of the intrusion before the fluids enter the permeable interior of the sheathed cylinder.

It is proposed here that all of the major features of midocean ridge hydrothermal systems reviewed above are related. Analyzing them together in the context of a particular conceptual model quantitatively defines the dimensions and critical characteristics of the deep (>1.5 km depth), higher temperature portions of the ridge axis hydrothermal system. In the model the 350°C isotherm marks the axis of the most permeable part of a thin (~3 m wide) permeable (~300 mD) flow and fluid-rock reaction zone that lies at the outside edge of the ~180-m-wide thermal boundary layer at the nearly vertical margin of the 1,200°C axial intrusion. The 350°C flow zone lies

between a ~2- and 7-km depth. Rapid permeability decrease with temperature generally keeps the flow zone from penetrating the thermal boundary layer of the axial intrusion, whereas heat balance and thermal buoyancy attract and concentrate it at the edge of the boundary layer. Calculations presented by Cathles (1983) show that in models where permeability drops at T > 350°C there is a natural tendency for flow to concentrate in a narrow ~350°C zone at the margin of an intrusion. Although very permeable, it is shown below that the relatively high fluid velocities in such a flow zone make it the most resistive part of the overall circulation path.

Because the 350°C flow zone is the most resistive link in the circulation loop, increases in flow zone permeability (as might easily be caused by magma withdrawal, thermal contraction in the thermal boundary layer, or pulses of magmatic volatiles expelled from the intrusion) can increase the discharge rate. Because permeability depends on the cube of fracture aperture or porosity, the large increases in flow zone permeability required to support megaplume rates of discharge are feasible. When the permeability increases significantly, the flow zone contracts to a small fraction of its former width and the heat content of the flow zone is emptied into a megaplume. No fluids are ponded, rather heat is stored in the rock matrix. The emptying of the flow zone thermal reservoir causes termination of the megaplume discharge. No mineral precipitation and resealing of a reservoir cap is required and the heat discharged in the megaplume provides a direct measure of the heat content (volume) of the flow zone. Since the width of the flow zone has simply contracted, the system returns to normal rates of discharge after the megaplume has discharged. No significant changes in the temperature of the system need occur. The fluid residence time is the parameter most dramatically changed before and after megaplume discharge.

Definition of the width and geometry of the flow zone and the width of the thermal boundary layer that separates it from the 1,200°C isotherm (the hot core of the axial intrusion) provides a context for analyzing the interaction between of the flow zone and its thermal boundary layer. Sudden cracking of the thermal boundary layer could draw 350°C seawater into a hot-enough environment to cause its segregation into a saline brine and a low-salinity vapor. Most of the vapor returns to the 350°C flow zone where it recondenses and dilutes the salinity of the flow zone fluids. The brine left behind in the boundary layer is later recovered when the flow zone migrates into the boundary layer (as it eventually must do). Cracking events could thus produce low-salinity discharges, and flow zone migration events could produce high-salinity discharges. The high-temperature Cl-rich veins with no halos observed in the Bushveld are direct evidence for the proposed thermal boundary layer cracking and phase segregation phenomena. The 350°C flow zone is the site of the most intensive fluid-rock interaction and the most likely source of base and precious metals that are deposited as massive sulfide on the sea floor. The nature and dynamics of the 350°C flow zone, and the fact that it fundamentally controls the operation of midocean ridge hydrothermal systems, is thus of particular relevance to economic geology.

It is shown below that the normal heat and fluid discharge rates observed at black smoker systems, the normal flow zone residence time, and the heat discharged during megaplume events define the thickness and porosity of the flow zone and the width of the thermal boundary layer separating the flow zone from the 1,200°C intrusion. General equations are developed but discussion is initially focused on a specific base case. Next, fracture and flow zone dynamics are considered and shown capable of producing the observed variations in discharge salinity. Field evidence from the Bushveld is discussed. Finally, variations from the base case and drilling and other tests of the model are considered, and field observations of potential value in massive sulfide exploration are identified.

The Capless Model

The system envisioned is illustrated in Figure 1. Inflow occurs to a distance from the ridge axis about equal to the depth of circulation (~7 km). The inflow is concentrated in a thin upflow zone (fz) of width Δr_{fz}, near the margin of a narrow magma chamber with its top lying a few kilometers beneath the sea floor. The height of the magma chamber is h, the thickness of the oceanic crust, H. A thermal boundary layer (tbl) of width ΔR_{tbl} separates the flow zone from the intrusion. The hydrothermal fluids move

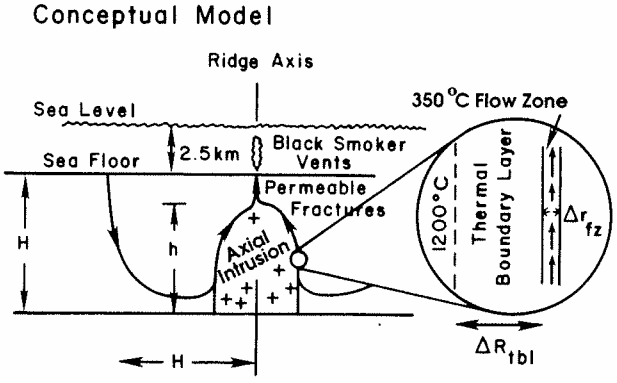

FIG. 1. A shematic of the ocean ridge hydrothermal system. Recharge occurs from near the ridge axis to a distance about equal to the thickness of the oceanic crust, H. The upward circulation path is a narrow 350°C flow zone at the outer margin of the thermal boundary layer of the axial intrusion.

from the top of the flow zone to the surface through fractures that parallel the ridge and lie very close to the ridge axis. The residence time of 350°C fluids in these fractures is short compared to their residence time in the more intimately and chaotically fractured rock in the flow zone. The fluids enter the flow zone at the base of the intrusion and elsewhere at temperatures below those at which significant fluid-rock interaction takes place (<150°C). Thus the residence time indicated by radioisotopic analysis of the vent fluids is the residence time of the fluids in the 350°C flow zone adjacent to the intrusion. In the discussion that follows it is assumed that the 350°C flow zone has a perimeter of 12.5 km and a height of 5 km for a total lateral area of 62.5 km^2. Geometrically this could represent two sides of a dike 5 km high and 6.25 km wide, or a cylindrical intrusion 4 km in diameter and 5 km high. Different intrusive geometries could be chosen provided the surface area of the intrusion that is exposed to hydrothermal fluids is kept at 62.5 km^2. The intrusion is considered to extend to Moho depths in order to satisfy near-ridge patterns of heat flow and be compatible with oxygen isotope alteration in ophiolites.

Mathematical analysis

Assuming, what later will be shown to be the case, that the main resistance to fluid circulation is the 350°C flow zone, the fluid velocity and residence time of the fluid in the flow zone can be easily calculated. The fluid mass flux is given by:

$$q_{fz} = \frac{k_{fz}\Delta\rho g}{\nu}, \tag{1}$$

where q_{fz} is the mass flux upward through the flow zone in g/cm^2 s, k_{fz} is the permeability of the flow zone in cm^2, $\Delta\rho$ is the difference in fluid density inside and outside the 350°C flow zone ($\sim$0.3 g/cm^3), g is the gravitational acceleration (1,000 cm/s^2), and ν is the fluid viscosity ($\sim 2 \times 10^{-3}$ cm^2/s for 350°C water). This formula assumes that cold water (e.g., normal geothermal gradient) hydrostatic pressures are maintained at the margin of the flow zone (e.g., Donaldson, 1968; Cathles, 1981).

The residence time of fluid in the 350°C flow zone equals the mass of fluid in the flow zone divided by the mass flux:

$$\tau_{fz} = \frac{\phi_{fz} h \rho}{q_{fz}}. \tag{2}$$

Here τ_{fz} is the residence time of fluid in the flow zone in seconds, ϕ_{fz} is the porosity of the flow zone, h is the length, essentially the height, of the flow zone in cm, and ρ is the density of the 350°C fluid in the flow zone ($\sim$0.7 g/cm^3).

If P is the perimeter of the flow zone around the magma body and Δr_{fz} the width of the 350°C flow zone (both in cm), the total discharge of the associated black smoker fields in g/s, Q, is:

$$Q = \Delta r_{fz} P q_{fz}. \tag{3}$$

The effective width, ΔR_{tbl}, of the thermal boundary layer separating the flow zone and magma may be estimated from the steady (nonmegaplume) thermal discharge associated with black smoker venting (= $QT_{vent}c$), the surface area of the flow zone facing the magma chamber, Ph, and the heat flux through the thermal boundary layer, $j_{tbl} = K\Delta T_{tbl}/\Delta R_{tbl}$. ΔT_{tbl} is the difference in temperature across the thermal boundary layer (= 1,200°–350° = 850°C), T_{vent} (= T_{fz}) is the temperature of black smoker venting (350°C), c is the heat capacity of water (1 cal/g – °C), Q is the total discharge rate of the black smoker field or fields fed by the magma chamber in g/s, K is the thermal conductivity of gabbro ($\sim 5 \times 10^{-3}$ cal/cm-s – °C; Clark, 1966), and ΔR_{tbl} is the width of the thermal boundary layer in cm. Heat balance requires that the thermal discharge equal the heat supplied across the conductive boundary layer:

$$j_{tbl} Ph = QT_{vent}c. \tag{4}$$

Substituting for j_{tbl} and solving for ΔR_{tbl} gives:

$$\Delta R_{tbl} = \frac{PhK\Delta T_{tbl}}{cT_{vent}Q}. \tag{5}$$

Note that the thermal boundary layer thickness, ΔR_{tbl}, is the effective thickness. It will undoubtedly vary in magnitude in the system (for example, be smaller at greater depths as would be expected from boundary layer theory), but its effective overall value must be that given by equation (5). If ΔR_{tbl} were less, more heat would be transferred to the flow zone than could be carried off by a discharge Q of 350°C water, and either more water or hotter water would have to discharge in contradiction to the stated situation.

Finally, if the heat discharged in a megaplume event, J, equals the heat content of the 350°C flow zone, then:

$$J = (T_{fz} - T_{amb})c_v \Delta r_{fz} Ph, \tag{6}$$

where T_{amb} is the average ambient temperature outside the flow zone ($\sim$100°C) and c_v is the heat capacity per unit volume of the flow zone ($\sim$0.54 cal/cm^3 – °C).

Equations (1) through (6) represent four independent (e.g., (1) and (3) are combined) equations that can be used to solve for the four principal unknowns of the hydrothermal system, ϕ_{fz}, k_{fz}, Δr_{fz}, and ΔR_{tbl} in terms of the principal measurable variables charac-

terizing the ridge hydrothermal system (τ_{fz}, Q, J, P, and h), i.e.:

$$\phi_{fz} = 6.075 \times 10^{12} \frac{Q[kg/s]}{J[cal]} \tau[yr] = 9.6, \quad (7)$$

$$k_{fz}[mD] = 1.28 \times 10^{16} \frac{Q[kg/s]}{J[cal]} h[km] = 336, \quad (8)$$

$$\Delta r_{fz}[m] = 7.4 \times 10^{-15} \frac{J[cal]}{P[km]h[km]} = 3.4, \quad (9)$$

$$\Delta R_{tbl}[m] = 438 \frac{P[km]h[km]}{Q[kg/s]} = 180, \quad (10)$$

$$q_{fz}[g/cm^2 - s] = 1.34 \times 10^{10} \frac{Q[kg/s]}{J[cal]} h[km] = 3.5 \times 10^{-4}. \quad (11)$$

The known parameter values indicated in the previous discussion have been substituted and the variables that remain have been expressed in convenient units. Equation (11) is added for completeness. The permeability units are millidarcies (= 10^{-11} cm^2) and are indicated by the notation mD. The numbers on the right of each equation are for the base case of h = 5 km, P = 12.5 km, Q = 150 kg/s, τ_{fz} = 3 yr, and J = 2.88×10^{16} cal.

Finally, the 350°C hydrothermal fluids discharging at the ridge axis recharge within a distance about equal to the depth of fluid circulation (e.g., Fehn et al., 1983), H, which is taken in the base case to be the thickness of the oceanic crust of 7 km. The permeability of the oceanic crust near the ridge axis will not control the rate hydrothermal circulation unless its average permeability is less than k_{fz} times the ratio of discharge to recharge areas:

$$k_{intake} > k_{fz}\Delta r_{fz}[km]P[km]/\pi H[km]^2 = 0.103 \text{ mD (base case)}. \quad (12)$$

In other words, intake will not restrict the rate of hydrothermal circulation unless the permeability of the oceanic crust near the ridge axis is less than ~0.1 mD.

Discussion of the mathematical model

The mathematical model described by equations (7) through (11) sets forth the conditions under which a ridge hydrothermal system can operate steadily at normal mass and heat discharge rates, yet be capable of discharging a megaplume of the dimensions observed on the Juan de Fuca Ridge if the permeability of the 350°C flow zone were suddenly increased. The parameters derived for the base case are all reasonable. The porosity, width, and permeability of the flow zone are plausible.

The near-ridge permeability of the ocean crust determines whether the 350°C flow zone is the most resistive part of the convective loop. Variations in surface heat flow 5 to 35 km from the Gallopagos Ridge produced by free convection to depths of ~3.5 km indicate crustal permeabilities of ~0.17 to 0.3 mD (see Cathles, 1981; COSOD II Working Group 3, 1987). The permeability of the crust within ~7 km of the ocean ridge thus exceeds 0.1 mD, and the main resistance to fluid circulation under normal black smoker discharge is the upwelling 350°C flow zone.

Estimates of the permeability very near the ridge are generally less than 3 to 10 mD (COSOD II Working Group 3, 1987), but these estimates assume that the restrictive part of the flow path is ocean crust, and thus, do not apply if the most restrictive part is the 350°C flow zone. The permeability very near the ridge could be substantially greater than 3 to 10 mD if the flow zone is the most resistive element in the circulation loop. Cann and Strens' (1989) megaplume model requires near-ridge permeabilities of 100 mD to 10 D, and much higher permeabilities in the discharge cylinder.

If the permeability very near the ridge axis were even one-tenth that of the 350°C flow zone, the system modeled here would have no difficulty obtaining a megaplume volume of water in 20 days. A pressure drop in the flow zone due to a sudden increase in its permeability will diffuse outward with time:

$$x[t] = 2(kt/\mu\phi c_\phi)^{0.5} = 3.6 \text{ km in 20 days for 30 mD}, \quad (13)$$

where x is the distance the pressure front has diffused from the flow zone, t is time in seconds, k is the permeability in cm^2, μ is the viscosity of the pore water in poise, ϕ the porosity of the crust near the ridge, and c_ϕ is the compressibility of the pore space. Taking $\phi c_\phi = 8.2 \times 10^{-12}$ cm^2/dyn (derived from figures for limestone and sandstone pore compressibility in Earlougher, 1977, appendix D), μ = 0.002 P, and k = 30 mD (10^{-10} cm^2), and substituting these values in equation (13) yields x [20 days] = 3.6 km. The fluid yield, ΔV_ϕ, from a pressure drop Δp in a volume of rock V is:

$$\Delta V_\phi = V\phi c_\phi \Delta p = 0.07 \text{ km}^3 \text{ for } \Delta p = 50 \text{ bars}. \quad (14)$$

If the average pressure drop in this zone is 50 bars, as it could easily be since the buoyancy gradient is ~30 bars per km over the 5-km vertical span of the intrusion for a total potential pressure reduction at the base of the intrusion of 150 bars, the yield of fluid from a volume V = Phx = 225 km^3 is 0.07 km^3, a volume of fluid similar to that discharged in the Juan de Fuca megaplume of 0.03 to 0.08 km^3 (Baker et al., 1989). If the permeability near the ridge is ~300 mD, the requisite volume could be obtained in 2 days. In 20 days and 300 mD the pressure drop would at least partly reach the sea floor (e.g., x = 6.1

km) and water could be drawn in from the ocean as well as the subsurface.

Finally it is quite reasonable that the permeability of the 350°C flow zone might increase by the factor of ~250 required by megaplume rates of discharge. The permeability of fractured rock is proportional to the cube of the effective flow porosity times the square of the fracture spacing or particle diameter for a large range of models (e.g., Kozeny-Carmen relationship, see Domenico and Schwartz, 1990, p. 76ff; generalization to turbulent flow, Bird et al., 1960, p. 197ff). The effective flow porosity for a fracture spacing of 10 cm and permeability of 336 mD is 3×10^{-6}. This effective flow porosity could easily be increased by a factor of 10, in which case the permeability would be increased by a factor of 1,000. Such increases in flow porosity could be induced by episodes of deflation in the magma chamber or by thermal contraction of the thermal boundary layer. For example, assuming a thermal expansion coefficient of $3.3 \times 10^{-5}°C^{-1}$ (Parsons and Slater, 1977), a 10°C cooling of the 180-m-wide thermal boundary layer could increase the porosity of a 3.6-m-wide flow zone by 1.6 percent. If just a fraction of this increase went to increasing flow porosity, the permeability could be increased far more than a factor of 10^3.

After megaplume discharge the system would return to approximately normal operation because the heat flux from the thermal boundary layer would remain substantially unchanged. If Q is unchanged, it can be seen from equations (1) and (3) that the width of the flow zone is reduced by the ratio of the permeability of the flow zone before and after the discharge event. The mass flux through the flow zone, q_{fz}, has increased by the same factor. The residence time of fluids in the flow zone has been greatly reduced, since it is unlikely ϕ_{fz} will increase in the now very narrow flow zone by more than a factor of 2 (and it cannot increase by more than a factor of 10 since it is initially ~10%), yet for megaplume discharge the permeability and mass flux must increase by 2.5 orders of magnitude. The main change before and after megaplume discharge will therefore be a very large (>25-fold) decrease in the residence time, τ_{fz}, of fluids in the 350°C flow zone.

The dynamics of the 350°C flow zone

Increased discharge could be caused by thermal contraction when the cracking front advances into the thermal boundary layer at the margin of an axial pluton, but increased discharge could occur at quite different times as well. For example, increased discharge might be associated with episodes of magma withdrawal, not cracking front advances. It is thus appropriate to separate formally the cracking front advances that lead to salinity variations in the flow zone from changes or movements of the 350°C flow zone that affect discharge rate. This does not mean that the two cannot occur simultaneously, just that they need not occur simultaneously.

Large thermal stresses develop in the thermal boundary layer where temperature decreases from 1,200° to 350°C over ~180 m. Thermal contraction stresses can intimately fracture the gabbro layer (Lister, 1983). When fracturing occurs in the thermal boundary layer, cracks penetrate toward the magma chamber at sonic velocity. Pore fluid will be drawn into much hotter rock rapidly enough that it will not at first be substantially heated. An instant later, however, contact with fracture walls will heat the water very close to the temperature of the surrounding rock. This is because the heat content of the rock is much greater than the heat required to raise 3.5 vol percent new water (the pore space that could be produced due to cooling from 1,200 to 350°C with a coefficient of thermal expansion of $3.3 \times 10^{-5}°C^{-1}$) to the local temperature of the rock. If the local environment is hot enough, heating of the seawater will cause it to separate into a high-salinity liquid phase and a low-salinity vapor phase. As shown below, the vapor phase will be expelled back toward the 350°C flow zone leaving behind a residual salt-rich liquid. At lower temperatures, the water simply thermally expands as a single phase and expels seawater back toward the 350°C flow zone. The temperature-pressure trajectory that separates simple thermal expansion from phase separation (the two-phase curve of seawater) is defined by the thermodynamic properties of water (Bischoff, and Rosenbauer, 1985; Bischoff and Pitzer, 1989).

Figure 2 illustrates the situation for a cross section of the thermal boundary layer from the top of a magma chamber at 1.5 km (400 bars) to 6.5 km (900 bars) depth beneath the sea floor. This figure is drawn assuming a normal hydrostatic gradient and shows that, depending on depth, fractures must extend more than 10 to 40 percent into the thermal boundary layer before a saline liquid will separate. As shown below, when this occurs most of the salt in the original seawater goes into a retained liquid and over 80 percent of the low-density vapor is expelled and recondenses in the cooler parts of the thermal boundary layer and 350°C flow zone. Thus to the right of the two-phase curve in Figure 2 the seawater is effectively stripped of its salt and returned to the zone to the left as relatively fresh water. If the salinities of water in the 350°C flow zone are to be reduced by 50 percent, the water returning from the right of the two-phase curve must be able to dilute both the seawater that has just been drawn into the cracks in the thermal boundary layer to the left of the two-phase curve and the water in the flow channel. Assuming the porosity associated with the new fractures in the thermal boundary layer does not change with dis-

Fluid Pressure, Bars

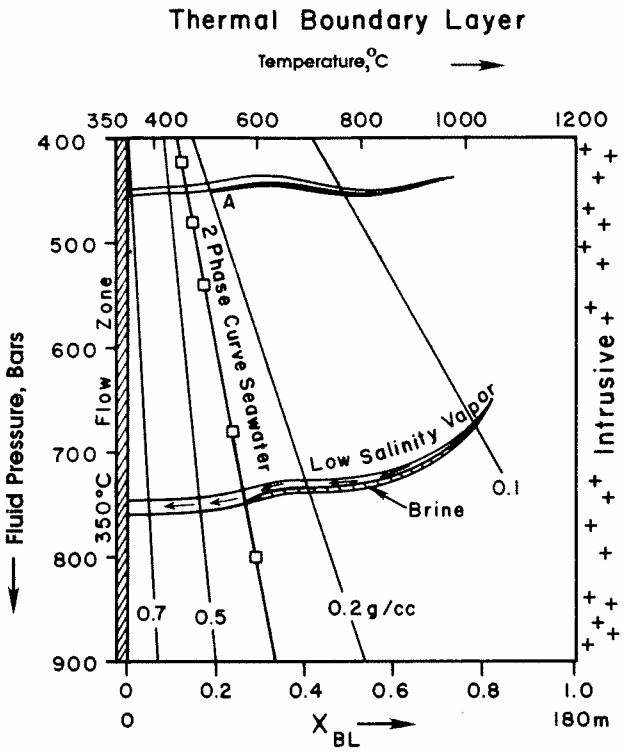

FIG. 2. Schematic illustration of temperature, pressure, and phases relations in the thermal boundary layer. The diagram assumes that open fractures communicate with the 350°C flow zone and uses a cold water hydrostatic gradient of 100 bars per km for the pressure axis. The temperature gradient across the thermal boundary layer is linear from 350°C at the flow zone to 1,200°C at the intrusion margin. The two-phase curve of seawater marks the distance from the flow zone at which seawater will separate into a brine and low-salinity vapor phase (Sourirajan and Kennedy, 1962). Isodensity lines to the left of the two-phase curve indicate the density of seawater (Bischoff and Rosenbauer, 1985, appendix 5). Isodensity lines to the right of the two-phase line indicate the density of pure water vapor (Burnham et al., 1966). The small salt content of the vapor will not change these densities significantly. As discussed in the text, 350°C seawater will be drawn into the fractures at sonic velocities without heating by a fracturing event and then will be heated to the temperature of the local environment. The result will be that to the right of the two-phase line the seawater will separate into a brine and vapor phase. The brine will be retained in the thermal boundary layer fractures since it occupies only about 10 vol percent of the fractures. Most of the vapor will be expelled to the left of the two-phase curve and into the flow zone where it will recondense and dilute the salinity of the pore waters. Point A is specifically discussed in the text to illustrate these points.

tance from the flow zone, this means the fractures must extend a distance into the thermal boundary layer equal to $\Delta r_{fz}(\phi_{fz}/\phi_{tbl})$ plus twice the distance between the two-phase curve and the flow zone. Here ϕ_{tbl} is the porosity of the new fractures in the thermal boundary layer and ϕ_{fz} is the porosity of the flow zone. Taking ϕ_{tbl} = 1 percent, ϕ_{fz} = 10 percent, and Δr_{fz} = 3.6 m, the cracking zone must extend into the thermal boundary layer a distance equal to 36 m plus twice the distance between the flow zone and the two-phase line. From Figure 2 this means that a cracking front must extend about 70 percent of the way across the thermal boundary layer and penetrate to temperatures of about 950°C. If a cracking event of this magnitude occurred, the salinity of the flow zone adjacent to the advance would be reduced by ~50 percent. The low-salinity zone thus created would mix with other fluids in the flow zone and be erased unless the affected portion of the flow zone was an appreciable fraction of the whole. Thus, to be effective in decreasing salinity, excursions of the cracking front must occur at the same time throughout most of the thermal boundary layer associated with a black smoker field.

Simple calculations using data from Bischoff and Pitzer (1989), Bischoff and Rosenbauer (1985), Sourirajan and Kennedy (1962), and Burnham et al. (1969) illustrate the points made above. Consider a point A at 450 bars and 500°C just inside the two-phase line in Figure 2. At this point, shortly after fracturing, 6 wt percent of the original 3.2 wt percent NaCl seawater has been converted to a 44.5 wt percent NaCl brine and 94 wt percent has been converted to an 0.56 wt percent NaCl vapor. The specific volume of the brine is 2.19 cm^3/g and the vapor ~5 cm^3/g. The specific volume of the initial 350°C water at 450 bars is ~1.4 g/cm^3. Thus about 9.3 vol percent of the vein (assuming it does not close) is liquid (= $100 \times 0.06 \times 2.19/1.4$) and 80 percent of the vapor has been expelled toward the flow zone. Since most of the vein is vapor and the viscosity of vapor is much less than that of the brine, the vapor will be expelled easily with very little tendency to entrain and also expel the brine. Points closer to the intrusion (e.g., hotter) separate into lower salinity vapors of greater specific volume and more saline brines. The result is that there is a clean separation of brine and some vapor in the thermal boundary layer beyond the two-phase boundary in Figure 2. Furthermore, most of the vapor is expelled to condense in the cooler parts of the boundary layer and in the 350°C flow zone.

Excursions of the cracking front into the thermal boundary layer appear to be a very natural way to produce fluids with salinities that are lower than that of seawater as is observed at many midocean ridge hydrothermal systems. Excursions reduce the salinity in the flow zone by producing and storing a brine in the thermal boundary layer. The 350°C flow zone must migrate through the thermal boundary layer. Even if magma chambers were a steady-state feature of midocean ridges, their narrow dimensions would oblige the flow zone to migrate toward the ridge axis at the half-spreading rate of the ridge. However, magma chambers are not steady-state features of the

midocean ridge. As indicated in the review of the literature, black smoker systems remove heat at rates significantly greater than can be steadily supplied by sea-floor spreading. Magma chambers are therefore transient. The 350°C flow zone must migrate through the thermal boundary layer faster than the spreading rate, perhaps at times appreciably faster. When the 350°C flow zone migrates into the boundary layer, the brine stored there will be flushed, producing an increase in discharge salinity complimentary to the decrease produced by the excursion of the cracking front.

Confirming field observations

The idea that fractures can be rapidly created and filled with relatively cool (350°C) fluids which fractionate to a saline liquid and low-salinity vapor, and that these fractures are subsequently flushed by migration of the 350°C flow zone toward the ridge axis, receives strong support from observations that have been made on veins in the Bushveld. Schiffries and Skinner (1987) documents three stages or types of veins in the Bushveld gabbro:

1. Early high-temperature (>600°C) veins 0.5 to 5 cm wide that are continuous for more than 10 m along strike and have distributions such that 0.2- to 2-m lengths of such veins can be found in a square meter area. They thus have an occurrence density of 0.2 to 2 m^{-1}. These veins contain calcic amphiboles with >5 wt percent Cl and calcic plagioclase. The veins have no alteration halos and for this reason are difficult to see in the field, being best observed on fresh wave-cut surfaces. Their high-temperature formation is attested to by their amphibolite-grade mineral assemblage and by the fact they are cut by migmatites.
2. Middle-stage hydrothermal veins, formed at temperatures from 600° to 300°C, 0.5 to 5 cm wide, with an occurrence density of 0.2 to 2 m^{-1}, and commonly continuous for 20 m or more along strike. These veins contain hydrothermal clinopyroxene and fluid inclusions with halite daughters. They have white alteration halos about one-third the vein width.
3. Late-stage <300°C, 1-mm-wide veins with wide alteration halos and some halite fluid inclusions. These veins are highly irregular in occurrence density (10–100 m^{-1}), with the high occurrence densities associated with shears and occurrence densities <10 m^{-1} found between shears.

Such veins are exactly what is expected to be found from the preceding discussion. The brine-filled veins that cut into high-temperature parts of the thermal boundary layer might well precipitate Cl-rich amphiboles and form and heal so quickly that there is no time to develop diffusion-controlled alteration halos. Veins formed at somewhat lower temperatures in the less plastic parts of the thermal boundary layer might remain open long enough to form narrow halos. This would be expected if the veins are used as temporary brine repositories. Finally, the more permeable ~350°C flow zone should be highly fractured and highly altered because of the high fluid throughput. The intense alteration associated with the third-stage Bushveld veins, as well as their patchy distribution, suggests a narrow 350°C flow zone similar to that discussed above.

The vein widths and occurrence densities are appropriate for formation by thermal contraction. From the widths and occurrence densities cited by Schiffries and Skinner (1987), fracture porosities of 0.1 to 10 percent can be calculated for all three vein stages. These porosities could, on average, sum to the 3.5 percent fracture porosity that would be produced by thermal contraction during cooling from 1,200° and 350°C with a thermal contraction coefficient of $3.3 \times 10^{-5}°C^{-1}$. The porosity values determined from residence times and energy balance thus match with field observations remarkably well. The fact that the highly altered zones associated with Bushveld stage 3 veins are distinct from the other higher temperature veins suggests that cracking events are distinct from flow zone migration events.

Discussion

The conceptual model presented in Figure 1, and shown to be viable by simple calculations, differs from previous models in several regards. The upwelling zone at the margin of the axial intrusion is very narrow, only a few meters wide, and has a much greater depth (1.5–6.5 km) than that suggested by previous models. The Moho depth of fluid circulation is not required to explain megaplumes or chemical variations but is required to explain the low heat flow near ocean ridges and the isotopic alteration to Moho depths observed in ophiolites such as the Samail. The 350°C flow and fluid-rock interaction zone controls the hydrothermal circulation like a throttle. Because it is thin (~3.4 m wide) and adjacent to intrusive activity, it is vulnerable to tectonic perturbations that can affect its permeability and the salinity of pore fluids circulating through it. In particular, increases in its permeability can lead to increased rates of discharge and drawdown of the thermal reservoir represented by the flow zone itself. For large increases in permeability, most of the heat in the flow zone can be rapidly discharged in a megaplume event. Termination of megaplume discharge occurs not when mineral precipitation or other events reduces the permeability to previous levels (as required in the Cann and Strens' model, 1989) or when hot fluids stored in a reservoir are released (as in Baker et al.'s and other storage models) but rather when the thermal reservoir of the flow zone is depleted. In fact, the heat

discharged in a megaplume event provides a direct measure of the heat content (volume) of the 350°C flow zone. This is the basis of the analysis presented above. The main change expected after megaplume discharge is a dramatic reduction in residence time of the fluid.

The model is perhaps uniquely compatible with the complex chemical variations in vent chemistry that have been observed. By comparing trace elements in laboratory experiments and chemical analyses of ridge hydrothermal fluids, Berndt and Seyfried (1990) concluded that phase separation, phase segregation, remixing of the segregated phases, Cl mineral precipitation, and the interaction of all the fluids with rock occurs at midocean ridges. Leaching of trace elements appears to precede phase separation. Phase-separated fluids show less reaction with rock than fluids that have remained single phase. A good specific example of the chemical complexities is provided by the analysis of seven vent fluids from a 60-m-diam area on Axial Seamount, Juan de Fuca Ridge. The chlorinity of these fluids ranges from 33 to 116 percent that of seawater and there are large variations in their gas content. Butterfield et al. (1990) concluded that the variations in salinity and gas content could best be explained by the remixing of the vapor and brine components of a hydrothermal fluid of seawater origin that had undergone phase separation. The vapor component must chemically interact with rock and recover Si, Li, and B before remixing. The distribution of fluids proved difficult to explain, however. Higher salinity fluids are presently being discharged from the main vents with more diffuse discharge of low-salinity fluids in the surrounding areas (Fox, 1990). Phase separation models based on density or viscosity cannot explain this distribution, but phase separation via a complicated scenario of relative permeability effects might (Fox, 1990). The dilemma of finding a compelling physical model to, first, separate vapor and brine components, and later, allow their recombination is a generally recognized problem. Berndt and Seyfried (1990, p. 2243) state, for example: "It remains to be determined, however, how fluids of seawater origin can achieve conditions required for phase separation and how vapor and brine components can be incorporated systematically into the free flowing portions of some geothermal systems. How do fluids which eventually vent have time to re-equilibrate with the host mineral assemblage at similar reaction zone temperatures following mixing with a condensed brine or vapor phase . . . ?"

The model presented here offers a physically simple and geologically plausible way to produce the chemical complexities observed. The rapid changes in chemistry observed over small spatial distances suggest that any successful model must be capable of producing temporally rapid chemical changes in fluid salinity and chemistry. A model in which the hydrothermal system has direct access to the intrusion can produce abrupt changes more easily than can a model in which the intrusive heat and fresh rock source is shielded beneath a layer of convecting brine. If the chemistry of deeper fluids can be rapidly changed, the distribution of fluids observed in places like Axial Seamount can easily be explained. Suppose, for example, that the flow zone at Axial Seamount had earlier been filled with low-salinity fluids produced after a cracking episode, and had just recently migrated into the thermal boundary layer and become saline. The low-salinity fluids in the high-permeability and lowest residence time conduits to the most active vents would quickly be replaced with brines. This would take longer in the less permeable conduits in the surrounding areas. Low-salinity fluids would continue to discharge from these vents for some time after the larger vents started discharging brines. From the published evidence this is as good an explanation of the current situation at Axial Seamount as that offered by Butterfield et al. (1990) and Fox (1990). The explantation is simple because it involves only single-phase displacement of different salinity and requires only the ability to change the salinity of deep source fluids rapidly.

The capless model can explain some of the other chemical observations and inferences. It provides a simple way to separate and then variably recombine the vapor and brine components of reacted seawater. Most chemical reaction (as reflected in alteration halo abundance) occurs in the 350°C flow zone; there is ample opportunity for separated phases to reequilibrate with rock. At least some reaction with hot rock in the thermal boundary layer precedes phase separation, as implicated by Berndt and Seyfried's (1990) analysis. The volatiles produced by the high-temperature thermal boundary layer reactions will be returned to the 350°C flow zone along with the volatiles in the original fluid. Since 94 wt percent of the water which enters the thermal boundary layer and undergoes phase separation is recondensed, the volatile enrichment of the low-salinity product need not be greatly above original levels. The volatile enrichment will depend in considerable degree on the kinetics of gas generating reactions in the thermal boundary layer at temperatures >450°C. All phases react with the host, but it is possible that fluids passing through the flow zone during periods when cracking events are not occurring could have statistically longer residence times in the flow zone and thus show more chemical interaction with the host rocks as suggested by Berndt and Seyfried's analysis.

The model presented here allows many opportunities for chemical complexity because independent physical processes can (and likely will be) combined

in different ways (producing something similar to a chemical combination lock); for example, fluid-rock interaction occurs mainly in the 350°C flow zone. Increases in fluid-rock interaction and hence the highest concentration of elements leached from basalt will be related to advances of this flow zone into unaltered rock in the thermal boundary layer. High concentrations of volatiles and elements rapidly leachable from rock at T > 450°C will reflect cracking events, however. Excursions in He/heat ratio are best explained in this way, for example (Baker and Lupton, 1990). Cracking events need not occur at the same time as movements of the flow zone, although the two could occur together. Increases in discharge salinity are related to migration of the flow zone, but the salinity will be flushed out immediately upon migration whereas the consequences of rock alteration in the newly established flow zone will take some time to develop. Increases in volatiles such as CO_2 could be introduced by magmatic volatiles and hence be related to magma chamber events independent of thermal boundary layer cracking or flow zone migration. Finally, discharge of the all these fluids and the amount of mixing en route to the surface will depend on the flow pathway. Slightly different residence times in different pathways will allow very different fluids to discharge simultaneously. Slightly different combinations of these physical processes can lead to great chemical complexity. The observed complexity supports the model.

Equations (7) through (11) show the dependencies of the model. For example, equation (7) shows that, for a given ratio of normal to megaplume discharge (Q/J), the fluid residence time, τ, provides a direct measure of flow zone porosity, ϕ_{fz}. If, for example, the residence time of fluids on the Juan de Fuca Ridge prior to megaplume discharge was 1 rather than 3 days, the porosity of the flow zone there would be 3.3 percent rather than 9.6 percent. It should be emphasized that the base case premegaplume residence time of 3 days is only a very rough estimate of the residence time appropriate for the Juan de Fuca megaplume area because the residence estimate was obtained by Kadko and Moore (1988) for a hydrothermal system on the Endeavour Ridge, not the Cleft segment of the Juan de Fuca Ridge. It should also be noted that after megaplume discharge, the residence time of fluids in the system will be very much reduced, and in fact, discharge of another megaplume will not be possible until the permeability of the flow zone has decreased and the flow zone has increased its width to premegaplume values of ~3 m. Equation (8) shows that, under the same constraint of constant (Q/J), the permeability of the flow zone, k_{fz}, is directly proportional to its height h. A flow zone half as high need have only half the permeability. If Q/J is reduced, so are both ϕ_{fz} and k_{fz}.

For a specified flow zone area Ph, the width of the flow zone (eq. 9) is directly measured by the heat discharged in a megaplume event, J, and the width of the thermal boundary layer is measured by the normal (nonmegaplume) discharge rate, Q. These relations are shown by equations (9) and (10). If the area of the flow zone were half the 62.5 km^2 assumed in the base case, the width of the flow zone could be twice the base case value (to maintain the same volume and the capability of supporting the observed megaplume discharge), and the width of the thermal boundary layer would be half the base case (to supply the nonmegaplume thermal output).

The model is strongly integrated and as a result many of its components will tend to succeed or fail together. For example, the narrow 350°C flow zone suggested by the short isotopic residence time of vent fluids is also required if substantial variations in discharge salinity are to be produced by cracking and flushing the thermal boundary layer. If the flow zone had a larger fluid volume, its salinity could not be changed by the volumes of water that could be reasonably supplied from the thermal boundary layer. If fluids are to be made available for megaplume discharges by the pressure drops that could be produced when the permeability of the 350°C flow zone is dramatically increased, at least ~30-mD permeabilities must extend several kilometers from the 350°C flow zone.

The conceptual model, as quantified in equations (7) through (10), can be tested by drilling. All the parameters on the left of these equations are in principle measurable by drilling. Drilling could provide a direct measure of flow zone porosity, permeability, and thickness, and a direct measure of the thickness of the thermal boundary layer, for example. All the variables on the right except P and h can be determined for a particular hydrothermal system by observing its performance before and after a megaplume event. An estimate of P and h can be made from seismic surveys with heat flow and isotopic constraints. If the theory presented here is close to correct, the values of ϕ_{fz}, k_{fz}, Δr_{fz}, and ΔR_{tbl} in the Cleft segment of the Juan de Fuca hydrothermal system, and perhaps in similar hydrothermal systems on other ridges, should be close to those presented in equations (7) through (10). High permeability near the ridge at depths > 2 km, a very narrow 350°C flow zone adjacent to the axial intrusion, and a reduction in the residence time of fluids after a discharge event by a factor about equal to the increase in permeability of the flow zone that caused the event are predictions that seem particularly testable.

The quantified conceptual model also indicates some field observations that might be useful in massive sulfide exploration. Large massive sulfide deposits should be produced by 350°C flow zones with

a large area (= Ph). Field observation of ϕ_{fz}, k_{fz}, Δr_{fz}, and ΔR_{tbl} might be possible. The product of equations (8), (9), and (10) yields:

$$2.4 \times 10^{-5} k_{fz}[mD] \Delta r_{fz}[m] \Delta R_{tbl}[m] = h[km]. \quad (15)$$

The perimeter of the flow zone and its depth extent are related, in particular $P = \sim 2\ h^2$. Thus, measuring the product of flow permeability, flow zone thickness, and thermal boundary layer thickness, as indicated by equation (15), could provide a direct measure of the area of the intrusion exposed to interaction with hydrothermal fluids and possibly a direct measure of the size of massive sulfide deposit that might be discovered in an area.

Megaplume discharge is probably unfavorable to massive sulfide accumulation because heat and minerals will be vented rapidly and spread over a very broad area of the sea floor. Megaplume events will promote jumps in the 350°C flow zone because of their tendency to cool the edge of the intrusion and produce extra thermal stresses. Nearly continuous (less patchy) stage 3 Bushveld-type veining would be a favorable indicator both because it suggests there has been no megaplume discharge and because it indicates that metals have been removed from a high percentage of the intrusion.

In conclusion, the simple conceptual model presented appears capable of explaining the normal and megaplume behavior of midocean ridge hydrothermal systems and variations in the salinity and chemistry of their discharge. The model makes predictions that are testable by drilling the 350°C flow zone and boundary layer of an ocean ridge hydrothermal system. The model identifies operational parameters that constrain the characteristics of ridge hydrothermal systems, notably the residence time of the fluid in the flow zone, the megaplume discharge, and the normal discharge rate, and identifies some new field measurements that may be useful in massive sulfide exploration.

Acknowledgments

The manuscript was improved by useful comments from three *Economic Geology* reviewers. The chemistry benefited from correspondence with Michael Berndt. The ideas presented, although very different, developed as the result of controversies surrounding the publication of Cann and Strens (1989) in which I became indirectly involved as an arbiter. I thank all parties for the stimulation the discussion produced. I also thank Steve Scott and Peter Rona for organizing the symposium that instigated preparation of this paper.

REFERENCES

Baker, E. T., and Lupton, J. E., 1990, Changes in submarine ^3He/heat ratios as an indicator of magmatic/teconic activity: Nature, v. 346, p. 556–558.

Baker, E. T., Massoth, G. J., and Freely, R. A., 1987, Cataclysmic hydrothermal venting on the Juan de Fuca Ridge: Nature, v. 329, p. 149–151.

Baker, E. T., Lavelle, J. W., Feely, R. A., Massoth, G. J., and Walker, S. L., 1989, Episodic venting of hydrothermal fluids from the Juan de Fuca Ridge: Journal of Geophysical Research, v. 94, p. 9237–9250.

Berndt, M. E., and Seyfried, W. E., 1990, Boron, bromine, and other trace elements as clues to the fate of chlorine in midocean ridge vent fluids: Geochimica et Cosmochimica Acta, v. 54, p. 2235–2245.

Bird, R. B., Stewart, W. E., and Lightfoot, E. N., 1960, Transport phenomena: New York, John Wiley, 780 p.

Bischoff, J. L., 1989, Salinity variations in submarine hydrothermal systems by layered double-diffusive convection: Journal of Geology, v. 97, p. 613–623.

Bischoff, J. L., and Pitzer, K. S., 1989, Liquid-vapor relations for the system NaCl-H_2O: Summary of the P-T-x surface from 300 to 500°C: American Journal of Science, v. 289, p. 217-248.

Bischoff, J. L., and Rosenbauer, R. J., 1985, An empirical equation of state for hydrothermal seawater (3.2 percent NaCl): American Journal of Science, v. 285, p. 725–763.

—— 1989, Salinity variations in submarine hydrothermal systems by layered double-diffusive convection: Journal of Geology, v. 97, p. 613–623.

Burnham, C. W., Holloway, J. R., and Davis, N. F., 1969, Thermodynamic properties of water to 1000°C and 10,000 bars: Geological Society of America Special Paper 132, 96 p.

Butterfield, D. A., Massoth, G. J., McDuff, R. E., Lupton, J. E., and Lilley, M. D., 1990, Geochemistry of hydrothermal fluids from Axial Seamount hydrothermal emissions study vent field, Juan de Fuca Ridge: Subseafloor boiling and subsequent fluid-rock interaction: Journal of Geophysical Research, v. 95, p. 12895–12921.

Campbell, A. C., Bowers, T. S., Measures, C. I., Falkner, K. K., Khadem, M., and Edmond, J. M., 1988a, A time series of vent fluid compositions from 21°N, East Pacific Rise (1979, 1981, 1985), and the Guaymas basin, Gulf of California (1982, 1985): Journal of Geophysical Research, v. 93, p. 4535-4549.

Campbell, A. C., Palmer, M. R., Bowers, T. S., Edmond, J. M., Lawrence, J. R., Casey, J. F., Thompson, G., Humphris, S., Rona, P., and Karson, J.A., 1988b, Chemistry of hot springs on the Mid-Atlantic Ridge: Nature, v. 335, p. 514–519.

Cann, J. R., and Strens, M. R., 1989, Modeling periodic megaplume emission by black smoker systems: Journal of Geophysical Research, v. 94, p. 12,227–12,237.

Cathles, L. M., 1981, Fluid flow and genesis of hydrothermal ore deposits: ECONOMIC GEOLOGY 75TH ANNIVERSARY VOLUME, p. 424-457.

—— 1983, An analysis of the hydrothermal system responsible for massive sulfide deposition in the Hokuroku basin of Japan: ECONOMIC GEOLOGY MONOGRAPH 5, p. 439–487.

Clark, S. P., 1966, Thermal conductivity: Geological Society of America Memoir 97, p. 459–482.

Converse, D. R., Holland, H. D., and Edmond, J. M., 1984, Flow rates in the axial hot springs of the East Pacific Rise (21°N): Implications for the heat budget and the formation of massive sulfide deposits: Earth and Planetary Science Letters, v. 69, p. 159–175.

COSOD II Working Group 3, 1987, Fluid circulation in the crust and the global geochemical budget, *in* Report of the Second Conference on Scientific Ocean Drilling (COSOD II): Strasbourg, France, Joint Oceanographic Institutions and European Science Foundation, p. 67–86.

Dietrick, R. S., et al., 1987, Multi-channel seismic imaging of a crustal magma chamber along the East Pacific Rise: Nature, v. 326, p. 35–41.

Domenico, P. A., and Schwartz, F. W., 1990, Physical and chemical hydrogeology: New York, John Wiley, 824 p.

Donaldson, I. G., 1968, The flow of steam-water mixtures through permeable beds: A simple simulation of a natural undisturbed hydrothermal region: New Zealand Journal of Science, v. 11, p. 3–23.

Earlougher, R. C., 1977, Advances in well test analysis: Society of Petroleum Engineers Monograph 5, 264 p.

Fehn, U., Green, K. E., Von Herzen, R. P., and Cathles, L. M., 1983, Numerical models for the hydrothermal field at the Galapagos spreading center: Journal of Geophysical Research, v. 88, p. 1033–1048.

Fox, C. G., 1990, Consequences of phase separation on the distribution of hydrothermal fluids at ASHES vent field, Axial volcano, Juan de Fuca Ridge: Journal of Geophysical Research, v. 95, p. 12923–12926.

Francheteau, J., and Ballard, R. D., 1983, The East Pacific Rise near 21°N, 13°S, and 20°S: Inferences for along-strike variability of axial processes of the midocean ridge: Earth and Planetary Science Letters, v. 64, p. 93–116.

Gregory, R. T., and Taylor, H. P., 1981, An oxygen isotope profile in a section of Cretaceous oceanic crust, Samail Ophiolite, Oman: Evidence for $\delta^{18}O$ buffering of the oceans by deep (>5 km) seawater-hydrothermal circulation at midocean ridges: Journal of Geophysical Research, v. 86, p. 2737–2755.

Kadko, D., and Moore, W., 1988, Radiochemical constraints on the crustal residence time of submarine hydrothermal fluids: Endeavour Ridge: Geochimica et Cosmochimica Acta, v. 52, p. 659–668.

Kelly, D. S., and Delaney, J. R., 1987, Two-phase separation and fracturing in midocean ridge gabbros at temperatures greater than 700°C: Earth and Planetary Science Letters, v. 83, p. 53–66.

Lister, C. R. B., 1983, The basic physics of water penetration into hot rocks, *in* Rona, P. A., Bostrom, K, Laubier, L., and Smith, K. L., eds., Hydrothermal processes at seafloor spreading centers: New York, Plenum Press, p. 141-168.

Macdonald, K. C., 1989, Anatomy of the magma reservoir: Nature, v. 339, p. 178–179.

Macdonald, K. C., Becker, K., Speiss, F. N., and Ballard, R.D., 1980, Hydrothermal heat flux of the "black smoker" vents of the East Pacific Rise: Earth and Planetary Science Letters, v. 48, p. 1–7.

McClain, J. S., Orcutt, J. A., and Burnett, M., 1985, The East Pacific Rise in cross section: A seismic model: Journal of Geophysical Research, v. 90, p. 8627–8639.

Morton, J. L., and Sleep, N. H., 1985, A mid-ocean ridge thermal model: Constraints on the volume of axial hydrothermal heat flux: Journal of Geophysical Research, v. 90, p. 11345-11353.

Parsons, B., and Sclater, J. G., 1977, An analysis of the variation of ocean floor bathymetry and heat flow with age: Journal of Geophysical Research, v. 82, p. 803–827.

Pisutha-Arnond, V., and Ohmoto, H., 1983, Thermal history, and chemical and isotopic compositions of the ore-forming fluids responsible for the kuroko massive sulfide deposits in the Hokuroku district of Japan: ECONOMIC GEOLOGY MONOGRAPH, 5, p. 523–558.

Rona, P. A., 1988, Hydrothermal mineralization at ocean ridges: Canadian Mineralogist, v. 26, p. 431–465.

Schiffries, C. M., and Skinner, B. J., 1987, The Bushveld hydrothermal system: Field and petrologic evidence: American Journal of Science, v. 287, p. 566–595.

Sourirajan, S., and Kennedy, G. C., 1962, The system H_2O-NaCl at elevated temperatures and pressures: American Journal of Science, v. 260, p. 115–141.

Tivey, M. K., Olson, L. O., Miller, V. W., and Light, R. D., 1990, Temperature measurements during initiation and growth of a black smoker chimney: Nature, v. 356, p. 51–54.

Vanko, D. A., 1986, High-chlorine amphiboles from oceanic rocks: Products of highly saline hydrothermal fluids?: American Mineralogist, v. 71, p. 51–59.

Von Damm, K.L., 1990, Seafloor hydrothermal activity: black smoker chemistry and chimneys: Annual Review of Earth and Planetary Sciences, v. 18, p. 173–204.